Supplementary Information (SI) for Journal of Materials Chemistry A.
This journal is © The Royal Society of Chemistry 2025

Supplementary document

Revolutionizing polymeric framework with integrated aluminium fragment for superior water decontamination empowered by statistical modeling approach

Shraddha Shukla[†a], Anil R. Gupta[a†], Surjit Bhai Ratnakar[b], Biswajit Ganguly[b†], Pankaj D. Indurkar[a†*], Saroj Sharma[a†*]

[a]Membrane Science & Separation Technology Division, CSIR-Central Salt & Marine Chemicals Research Institute, G. B. Marg, Bhavnagar-364002, Gujarat, India.
[b]Analytical And Environmental Science Division And Centralized Instrument Facility, CSIR-Central Salt & Marine Chemicals Research Institute, G. B. Marg, Bhavnagar-364002, Gujarat, India.
†Academy of Scientific and Innovative Research (AcSIR), Ghaziabad-201002, India.
*E-mail: sarojs@csmcri.res.in; saroj.sharma23@gmail.com, Tel: +91-278-2567700

S1. Analytical measurements and methods for analysis

The physicochemical properties of pAlTMA were investigated using a variety of measurement techniques. Various instrumentation techniques were used to investigate the physicochemical properties of p[AlTMA]. XRD instrument (Empyrean-PANalytical) equipped with Cu K radiation (wavelength: 1.54 Å). Phase identification and indexing were conducted within the 2θ range of 5-90° using HighScore Plus 3.0 software. The surface morphology of the nanomaterials was investigated using scanning electron microscopy (SEM) coupled with energy dispersive X-ray (EDX) analysis, employing a JEOL JSM 7100F instrument and INCA software. Fourier-transform infrared (FTIR) spectroscopy, employing a Perkin Elmer GXFTIR spectrometer and PFSPRO software, was utilized to examine functional groups within the wavenumber range of 400 - 4000 cm^-1 using the KBr pellet technique. X-ray photoelectron spectroscopy (XPS) was employed to analyze surface chemistry, with data analyzed using XPS software. Inductively coupled plasma mass spectrometry (ICP-MS), utilizing a Thermofisher Scientific instrument (model no-ICAPRQ) and Qtegra ISDS software (version 2.8.3170.309), was employed for determining the concentration of arsenic ions. The concentration of fluoride was measured utilizing a specialized ion sensor electrode designed for selective detection. To mitigate interference from other ions, samples were treated with TISAB I buffer solution containing CDTA.

S2. *Batch adsorption experiments*

The laboratory scale experiments of batch adsorption involved utilizing freshly prepared As(V), As(III) and F^- ions solution (50 ml), wherein various parameters were systematically varied. The different concentrations of As(V), As(III) and F^- ions solutions were

achieved by diluting a specific quantity of a prepared stock solution with a concentration of 1000 mgL^{-1}. The batch adsorption experiments incorporated varying the parameters, including adsorbent dose ranging from 50 to 300 mgL^{-1}, pH ranging from 3 to 10, concentration ranging from 0.05 to 0.25 mgL^{-1} for As(V) and As(III), while 5 to 50 mgL^{-1} for F^- ions, and time ranging from 10 to 180 minutes. All the adsorption experiments of arsenic and fluoride were implemented as per the Table S1 and S2, respectively. The 10 ml of sample solution collected in the vail after adsorption experiment using nylon syringe filter (0.22 mm). The ion-selective electrode was used to evaluate the filtered fluoride supernatant. To prevent interference from other ions, the samples were treated with a TISAB I buffer solution containing CDTA. Although, the filtered arsenic solution was analysed by ICP-MS instruments. The performance of pAlTMA adsorbent was examined by the amount of As (V), As(III), and F^- ions adsorbed and equilibrium adsorption capacity.

S3. *Adsorption kinetic models*

Adsorption kinetic models are mathematical expressions used to describe the rate at which adsorption processes occur over time. These models help in understanding and predicting the dynamic behavior of adsorption systems. The kinetics of As(V), As(III) and F^- ions removal were investigated using three widely recognized empirical kinetic models viz. Pseudo first order model (Eq. 5), the Pseudo second order model (Eq. 6), and the Elovich model (Eq. 7) .

$$q_t = q_e\left(1 - e^{-k_f t}\right) \tag{5}$$

$$q_t = \frac{q_e^2 k_s t}{1 + q_e k_s t} \tag{6}$$

$$q_t = \frac{1}{\beta}\ln(\alpha\beta) + \frac{1}{\beta}\ln(t) \tag{7}$$

In this equation, q_t and q_e represent the amount of adsorbed As(V), As(III), and F^- ions (mg g^{-1}) at time t (min) and equilibrium, respectively. The rate constants of pseudo-first and pseudo-second order are represented by k_f (1/min) and k_s (1/min), respectively. Moreover, α (mg g^{-1} min) and β (g mg^{-1}) are the constants for Elovich model.

S4. *Adsorption isotherm models*

Adsorption isotherm models are mathematical representations that describe the distribution of adsorbate molecules onto adsorbent surfaces at equilibrium conditions. The experimental data were employed to analyse Langmuir (Eq. 8), Freundlich (Eq. 10), Dubinin-

Radushkevich (D-R) (Eq. 11) and Temkin (Eq.12) isotherm models. These isotherm models provide insights into the adsorption mechanism, surface properties, and the maximum adsorption capacity of the adsorbent AlTMA. The adsorption behavior may be described using a dimensionless equilibrium parameter (RL) (Eq. 9). The fitting experimental data to these models determine the best-fitting isotherm and extracted relevant parameters for a better understanding of the adsorption process.

$$q_e = \frac{k_L q_{max} C_e}{1 + k_L C_e} \quad (8)$$

$$R_L = \frac{1}{1 + k_L C_0} \quad (9)$$

$$q_e = k_F C_e^{1/n} \quad (10)$$

$$q_e = q_d \exp(-B_{DR}\varepsilon^2) \quad (11)$$

$$q_e = B \ln A + B \ln C_e \quad (12)$$

Where, q_e (mg/g) is the adsorbent-phase concentration of adsorbate at equilibrium, C_e (mgL^{-1}) is the aqueous phase concentration of adsorbate at equilibrium, k_L is the constant relating to the binding site's affinity, q_{max} (mg g^{-1}) is the maximum (F^-/As)ions adsorption capacity per unit weight of pAlTMA at C_e. The constant k_F (mg g^{-1}) represents the relative adsorption capacity of the adsorbent. 1/n is the adsorption intensity and larger fractional values of 1/n indicate that the system has strong adsorption forces. q_d (mg g^{-1}) is the amount of Hg(II) ions adsorbed per unit doses, B_{DR} $(mol/KJ)^2$ is the sorption energy constant.

Table S1 RSM-CCD output for As(V) and As(III) removal using AlTMA adsorbent

		Factor 1	Factor 2	Factor 3	Factor 4	Respons e 1		Respons e 2	
Std	Run	A: Adsorbent dose	B:pH	C:Concentr ation	D:Time	As(III) removal	Predicted As(III) removal	As(V) removal	Predicted As(V) removal
		mg/L		mg/L	min	%	%	%	%
29	1	300	6.5	0.15	95	94.2	94.20	98.4	98.76
2	2	50	6.5	0.15	95	74	74.47	77.6	78.57
13	3	300	3	0.25	10	36.3	36.64	48.2	45.41
27	4	50	10	0.25	10	23.4	25.21	35.2	34.17
26	5	175	6.5	0.15	95	86.1	87.90	94.5	91.76
5	6	50	3	0.25	10	33.9	31.73	38.6	38.61
24	7	175	6.5	0.15	95	86.2	87.90	94.4	91.76

19	8	300	3	0.05	10	76.2	73.17	79.5	78.06
12	9	175	6.5	0.15	95	89.6	87.90	90.8	91.76
15	10	50	3	0.05	10	58.4	59.73	64.6	64.89
30	11	175	10	0.15	95	77.2	73.19	81.8	80.04
7	12	300	3	0.05	180	96.3	97.11	99.2	100.43
9	13	50	10	0.05	10	53.7	51.19	67.5	65.37
28	14	50	10	0.25	180	57.8	58.09	58.1	59.01
17	15	175	6.5	0.15	10	57.9	60.73	63.8	69.22
6	16	175	3	0.15	95	72.4	76.89	79.8	82.90
18	17	175	6.5	0.15	95	90.4	87.90	93.5	91.76
23	18	300	10	0.25	180	82.8	84.10	86.3	86.21
1	19	300	10	0.5	10	58.6	61.20	73.8	74.07
4	20	175	6.5	0.15	95	90.1	87.90	90.8	91.76
20	21	50	10	0.05	180	59.4	61.69	62.6	65.58
21	22	50	3	0.25	180	53.5	53.53	60.8	60.73
3	23	50	3	0.05	180	60.7	59.15	64.3	62.37
14	24	175	6.5	0.25	95	79.4	79.25	80.7	80.76
8	25	175	6.5	0.15	95	86.4	87.90	90.6	91.76
16	26	175	6.5	0.05	95	98.7	99.32	99.1	100.37
25	27	300	10	0.05	180	96.8	96.23	99.7	99.16
11	28	175	6.5	0.15	180	91.5	89.14	96.9	92.82
10	29	300	10	0.25	10	27.9	26.70	35.1	36.50
22	30	300	3	0.25	180	83.2	82.96	90.8	92.40

Table S2 RSM-CCD output for fluoride removal using AlTMA adsorbent

		Factor 1	Factor 2	Factor 3	Factor 4	Response 1	
Std	Run	A:Adsorbent dose	B:pH	C:Concentration	D:Time	F removal	Predicted F removal
		mg/L		mg/L	min	%	%
23	1	50	6.5	27.5	95	78.9	75.25
5	2	50	10	50	10	19.1	20.15
26	3	300	3	50	10	29.6	32.25
22	4	300	3	5	10	54.9	52.07
24	5	300	10	5	180	93.1	94.13
1	6	175	6.5	5	95	92.9	90.38
9	7	175	6.5	27.5	95	74.1	73.70
13	8	175	6.5	27.5	95	73.4	73.70
30	9	300	6.5	27.5	95	80.7	81.52
11	10	175	10	27.5	95	64.8	62.12
4	11	300	3	5	180	98.6	98.43
3	12	300	10	50	180	68.1	67.30
20	13	50	3	50	10	29.9	28.70
18	14	300	3	50	180	76.6	75.91
19	15	300	10	5	10	43.4	45.51
29	16	175	6.5	27.5	10	40.9	39.04
6	17	50	3	50	180	58.3	57.07

16	18	50	10	50	180	48.1	50.76
15	19	175	6.5	50	95	63.6	63.28
17	20	50	3	5	180	85.2	87.14
28	21	50	10	5	10	51.3	51.82
2	22	175	6.5	27.5	180	78.5	77.53
21	23	50	3	5	10	54.4	56.08
7	24	175	6.5	27.5	95	70.1	73.70
12	25	300	10	50	10	23.5	21.39
25	26	175	6.5	27.5	95	70.4	73.70
8	27	175	6.5	27.5	95	71.1	73.70
10	28	50	10	5	180	86.9	85.13
14	29	175	3	27.5	95	68.7	68.55
27	30	175	6.5	27.5	95	74.6	73.70

Table S3. ANOVA analysis for the CCD model for As(V), As(III) and F^- ions

	Source	**Sum of Squares**	**df**	**Mean Square**	**F-value**	**p-value**	
	Model	11226.32	14	801.88	102.45	< 0.0001	significant
	A-Dose	1834.16	1	1834.16	234.33	< 0.0001	
	B-pH	36.69	1	36.69	4.69	0.0469	
	C-Conc	1730.68	1	1730.68	221.11	< 0.0001	
	D-Time	2506.32	1	2506.32	320.21	< 0.0001	
	AB	20.03	1	20.03	2.56	0.1306	
As (V)	AC	40.64	1	40.64	5.19	0.0377	
	AD	618.77	1	618.77	79.05	< 0.0001	
	BC	24.26	1	24.26	3.10	0.0987	
	BD	7.43	1	7.43	0.9487	0.3455	
	CD	606.39	1	606.39	77.47	< 0.0001	
	A^2	24.81	1	24.81	3.17	0.0952	
	B^2	274.59	1	274.59	35.08	< 0.0001	
	C^2	3.70	1	3.70	0.4725	0.5023	
	D^2	299.12	1	299.12	38.22	< 0.0001	
	Residual	117.41	15	7.83			
	Lack of Fit	99.43	10	9.94	2.77	0.1365	not significant
	Pure Error	17.97	5	3.59			
	Cor Total	11343.73	29				
	Model	13341.19	14	952.94	122.30	< 0.0001	significant
	A-Dose	1750.35	1	1750.35	224.64	< 0.0001	
	B-pH	61.60	1	61.60	7.91	0.0131	
	C-Conc	1812.02	1	1812.02	232.56	< 0.0001	
	D-Time	3632.36	1	3632.36	466.19	< 0.0001	
	AB	11.73	1	11.73	1.51	0.2387	
As(III)	AC	72.68	1	72.68	9.33	0.0080	
	AD	601.48	1	601.48	77.19	< 0.0001	
	BC	4.10	1	4.10	0.5263	0.4793	

	BD	122.66	1	122.66	15.74	0.0012	
	CD	500.64	1	500.64	64.25	< 0.0001	
	A^2	32.86	1	32.86	4.22	0.0579	
	B^2	428.58	1	428.58	55.00	< 0.0001	
	C^2	5.00	1	5.00	0.6412	0.4358	
	D^2	435.27	1	435.27	55.86	< 0.0001	
	Residual	116.87	15	7.79			
	Lack of Fit	94.84	10	9.48	2.15	0.2057	not significant
	Pure Error	22.03	5	4.41			
	Cor Total	13458.06	29				
	Model	12664.54	14	904.61	122.35	< 0.0001	significant
	A-Dose	176.72	1	176.72	23.90	0.0002	
	B-pH	186.25	1	186.25	25.19	0.0002	
	C-Conc	3304.85	1	3304.85	446.97	< 0.0001	
	D-Time	6666.28	1	6666.28	901.59	< 0.0001	
	AB	5.29	1	5.29	0.7155	0.4109	
	AC	57.00	1	57.00	7.71	0.0141	
	AD	234.09	1	234.09	31.66	< 0.0001	
F^-	BC	18.49	1	18.49	2.50	0.1346	
	BD	5.06	1	5.06	0.6847	0.4209	
	CD	7.29	1	7.29	0.9859	0.3365	
	A^2	56.87	1	56.87	7.69	0.0142	
	B^2	181.29	1	181.29	24.52	0.0002	
	C^2	25.47	1	25.47	3.44	0.0832	
	D^2	615.65	1	615.65	83.26	< 0.0001	
	Residual	110.91	15	7.39			
	Lack of Fit	91.28	10	9.13	2.33	0.1821	not significant
	Pure Error	19.63	5	3.93			
	Cor Total	12775.45	29				

3.3. Adsorption Study

3.3.1 Batch scale adsorption with single ions

***S5**. Effect of pH and Point of zero charge (pH_{pzc})*

The influence of solution pH on adsorption efficacy was examined by changing the pH of the solution from acidic to alkaline i.e., 2±0.2–10±0.2, at set experimental environments, such as dose of pALTMA: 0.250 g L^{-1}, rpm: 150, contact time: 120min, temp.:30±2.0^oC, and F^-: 10 mg L^{-1}. pH_{pzc} affects a number of features of suspension materials, including stability, interface with electrolytes, and ion exchange capacity. It is associated to the surface charge and pH of the substance. The ion-selective electrode was used to evaluate the filtered fluoride supernatant. The drift method was used to calculate pH_{pzc} of pAlTMA.

***S6**. Effect of co-existing ions*

It is observed that numerous interfering anions are present in natural ground or surface water such as phosphate (PO_4^{3-}), sulfate (SO_4^{2-}), bicarbonate (HCO_3^-), nitrate (NO_3^-), and chloride (Cl^-). It is observed that presence of these co-existing anions in water may impede the adsorption of arsenic and fluoride. Hence, in order investigate the impact of co-existing anions on the elimination of fluoride and arsenic with pAlTMA, a few anions such as Cl^-, NO_3^-, SO_4^{2-}, HCO_3^- and PO_4^{3-} are chosen separately. Coexisting anions concentration were maintained at 100 mg L^{-1} with fluoride at 10 mg L^{-1}, and arsenic at 0.2 mg L^{-1} in the solution.

***S7.** 3.3.2 Binary phase adsorption study*

The experiments on binary adsorption were carried out at varying experimental i.e., dose of pAlTMA, Feed concentration and pH of the medium

3.3.2.1 Effects of adsorbent's dose and feed concentration

The effect of varying dose of pAlTMA and feed concentration of arsenic and fluoride were employed to assess its performance in a mixed simulated solution (As: 0.2 mg L^{-1}, +F: 10 mg L^{-1}), while keeping other parameter fixed (pH: 7.0±0.2, temp.: 25 ± 2.0°C agitation speed rpm: 250 rpm, time: 210 minutes). The results suggest a synergistic interaction between fluoride and arsenic during the adsorption process in binary phase. In the first experiment, the performance was examined by varying dose of pAlTMA, in the fixed concentration binary solution (F^-+ As), and another parameter were also constant. It was observed that as the dose of pAlTMA increased from 0.05 to 0.15 g L^{-1}, the arsenic and fluoride removal efficacies rose sharply from 71.25% to 96.34% and 78.35% to 98.21% respectively. Upon further increasing the dose to 0.31 gL^{-1}, removal efficiencies reached 98.21% and 96.34% for fluoride and arsenic respectively [Fig. S1 (a,b)].

Next, set of experiment, the impact of feed concentration on the adsorption behaviour of arsenic and fluoride ions using pAlTMA was systematically investigated. Thus, the concentration of one ion was varied; while keeping the other constant to assess their interactive influence on the adsorbent's performance. Results revealed that with increasing concentrations of arsenic from 200–5000 µg L^{-1} with fixed concentration of fluoride (10 mg L^{-1}) led to a substantial enhancement in arsenic removal efficiency, from 57.32% to 96.31%. While with increasing concentrations of fluoride from 5-50 mg L^{-1}, with fixed concentration of arsenic (200 µg L^{-1}), the fluoride removal efficiency increased from 70.34% to 99.1%. The maximum adsorption capacities (q_{e_max}) for fluoride and arsenic were observed as 31.75 mg g^{-1} and 0.62 mg g^{-1}, respectively in binary phase medium. [Fig. S2 (a, b)].

These findings affirm pAlTMA's robust capacity to effectively remove both fluoride and arsenic, achieving compliance with WHO drinking water standards (F^-: ≤1.5 mg·L^{-1}; As: ≤10 µg·L^{-1}). Moreover, the results suggest a synergistic interaction between fluoride and arsenic during the adsorption process. Fluoride exhibited a more pronounced inhibitory effect on arsenic adsorption, likely due to increased ionic strength and competitive interactions for active sites. In contrast, the presence of arsenic notably enhanced fluoride removal, particularly at elevated arsenic concentrations, highlighting a complex interplay that influences adsorption dynamics.

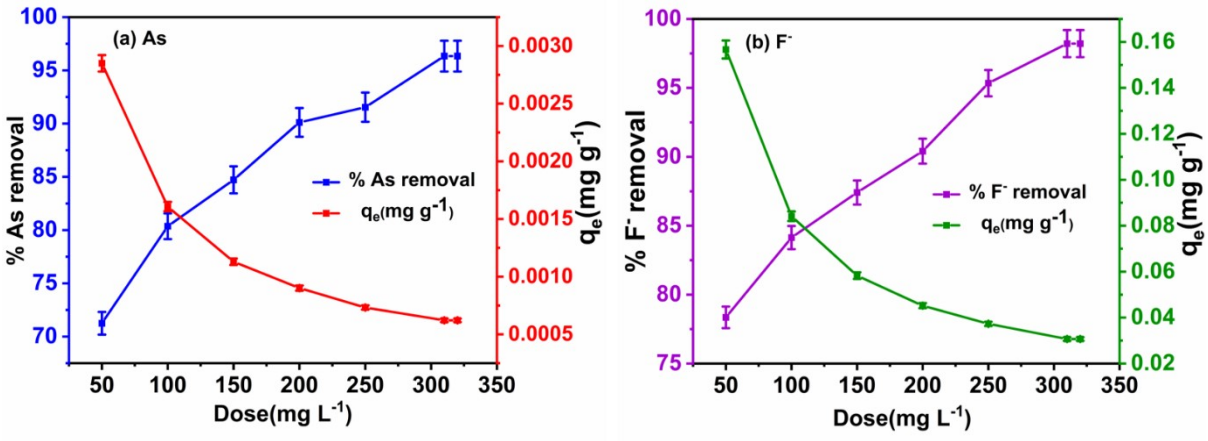

Fig. S1 Effect of dose on performance efficacy of pAlTMA (a) arsenic (b) fluoride with fixed binary phase (As: 0.2 mg L^{-1} +F^-: 10.0 mg L^{-1}), agitation time: 210 minutes, agitation rate: 250 rpm, pH: 7.0±0.2, adsorption temp.: 25 ± 2.0°C

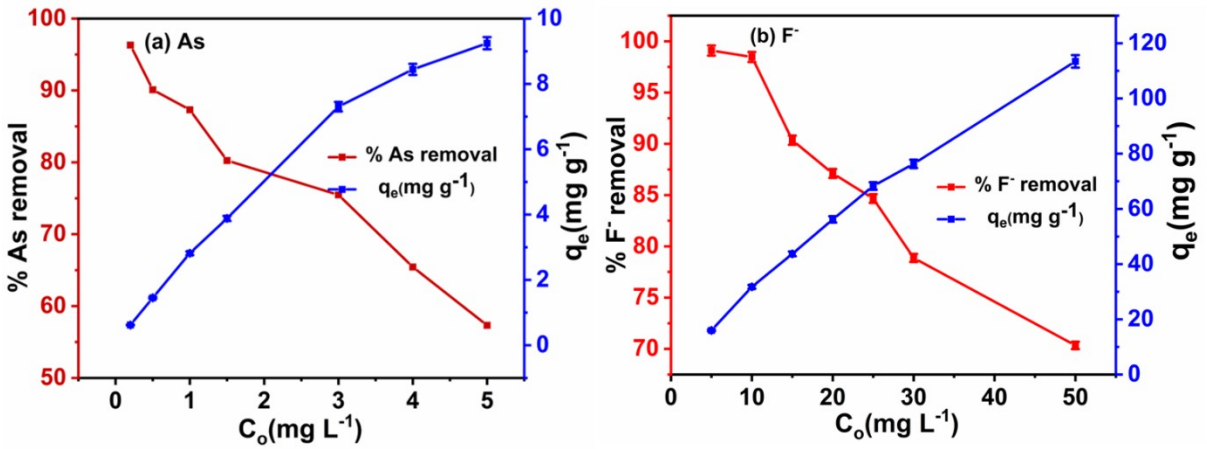

Fig. S2 Effect of concentration on performance efficacy of pAlTMA (a) arsenic (b) fluoride in binary phase with fixed quantity pAlTMA: 0.31 gL^{-1}, agitation time: 210 minutes, agitation rate: 250 rpm, pH: 7.0±0.2, adsorption temp.: 25 ± 2.0 °C

S8*. Regeneration, recapture and safety assessment*

Any material, which is able to bring down the operating expenses, whereas minimising maintenance costs would be ideal for field deployment. As a result, adsorption-desorption studies were conducted to determine the reusability of the produced adsorbent. After testing different eluting agents to desorb arsenic and fluoride under certain experimental settings, the eluting agent with the highest desorption effectiveness for the targeted ions was selected for the present work.

For safety assessment, the utilised pAlTMA from adsorption studies was investigated for TCLP test to establish if the spent spherical material was inert or dangerous about the leachability of Al in water. Hence, treated water samples were analysed by ICP-MS analysis to examine the presence of these ions in water samples.

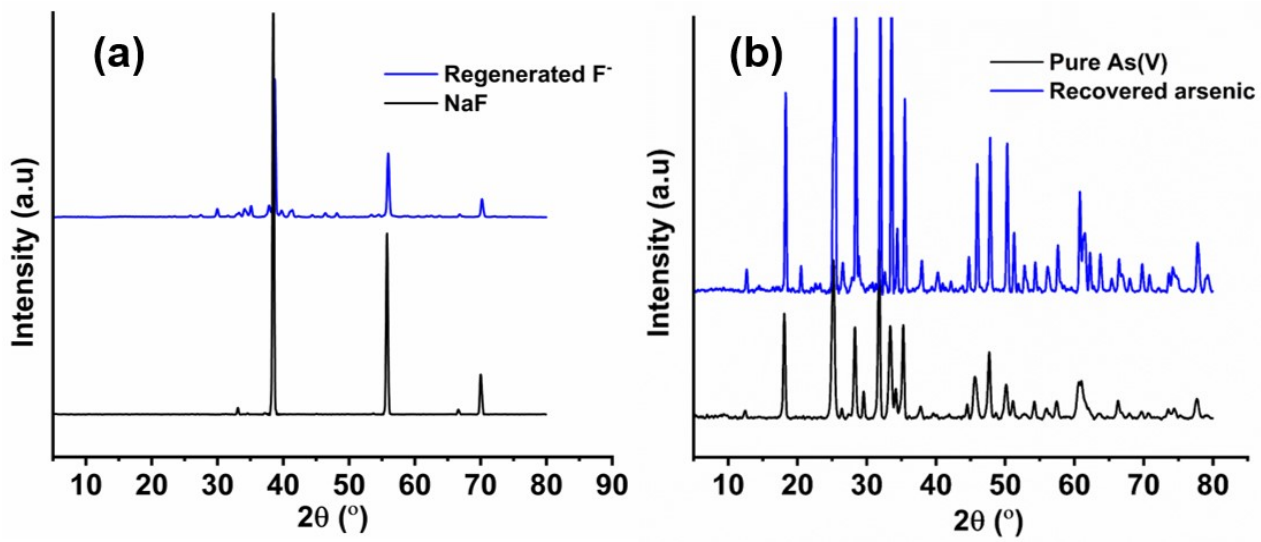

Fig. S3 XRD spectra of recovered salt of (a) fluoride and (b) arsenic.

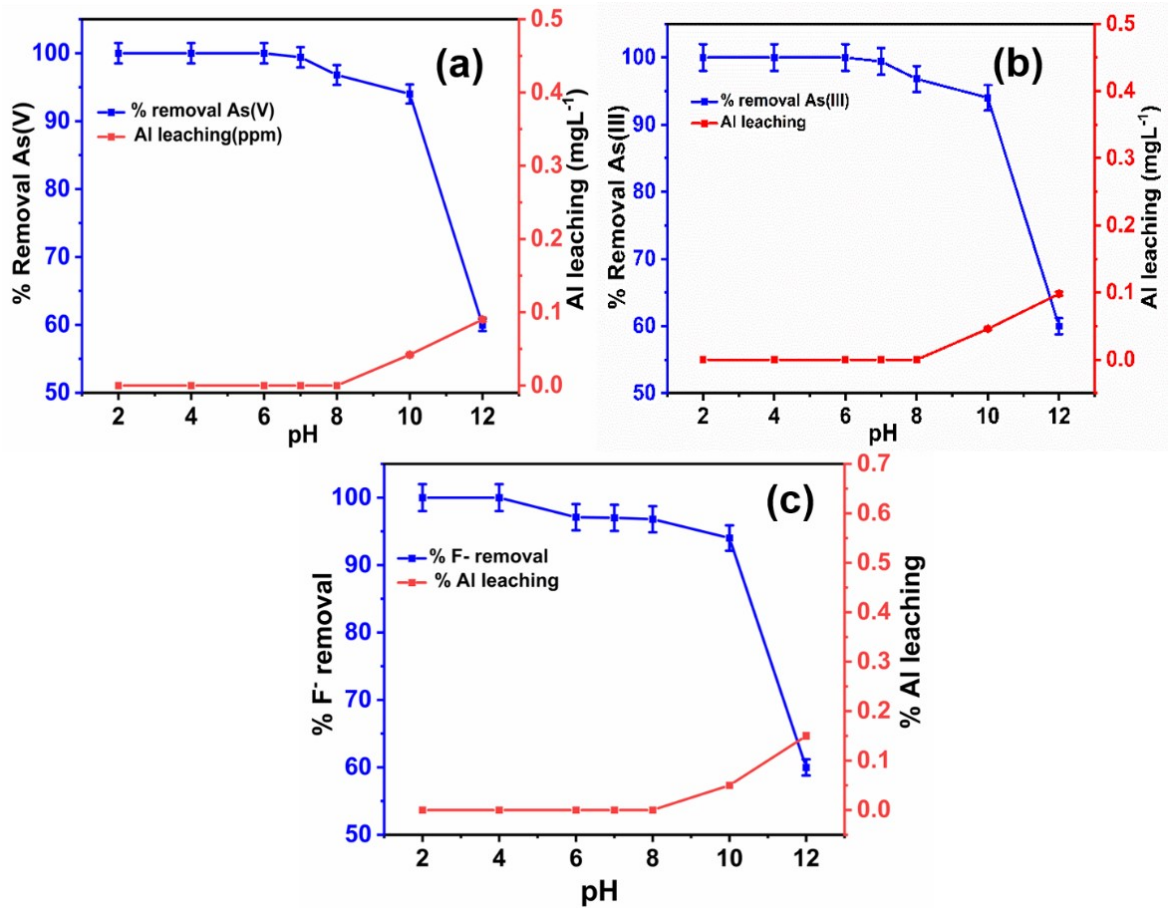

Fig. S4 Leaching study of pAlTMA at varying pH, Feed As(V)/As(III) : 0.175 mg L^{-1} , F^- : 10.5 mg L^{-1}, temp.: 298 K, pAlTMA dose: 298 mg L^{-1} for arsenic and 287 mg L^{-1} for fluoride.

Table S4 Kinetics data of AlTMA adsorbent for As(V), As(III) and F^- ions

Temperature (K)	**Pollutants**	**Parameters**								
			PFO			**PSO**			**Elovich**	
		k_f *(min^{-1})*	q_e *(mg g^{-1})*	R^2	k_s *(min^{-1})*	q_e *(mg g^{-1})*	R^2	α *(mg/g min)*	β *(g/mg)*	R^2
	As(V)	0.0178	0.4129	0.9564	0.0777	0.6243	0.9970	0.0681	8.7260	0.9917
288	**As(III)**	0.0219	0.6633	0.9493	0.0380	0.6585	0.9991	0.0379	7.2463	0.9966
	F^-	0.0196	23.396	0.9441	0.0016	37.921	0.9969	32.008	0.2045	0.9851
	As(V)	0.0172	0.4580	0.9363	0.0590	0.6124	0.9960	0.0689	8.8967	0.9906
298	**As(III)**	0.023	0.7685	0.9500	0.0264	0.6802	0.9979	0.0275	6.7796	0.9921
	F^-	0.0191	28.078	0.8208	0.0013	37.993	0.9934	20.616	0.1955	0.9725

	As(V)	0.0190	0.5983	0.8431	0.0375	0.6284	0.9951	0.0362	7.7345	0.9916
308	**As(III)**	0.0193	0.6399	0.9626	0.0210	0.6855	0.9979	0.0233	6.8166	0.9941
	F^-	0.0156	26.509	0.9450	0.0009	38.476	0.9912	7.6743	0.1644	0.9720
	As(V)	0.0184	0.6125	0.8010	0.0324	0.6240	0.9908	0.0309	7.7459	0.9890
318	**As(III)**	0.0182	0.6150	0.9368	0.0182	0.6773	0.9943	0.0205	7.0521	0.9953
	F^-	0.0143	27.796	0.9293	0.0008	38.729	0.9872	4.9707	0.1517	0.9736

Table S5 Arsenic containing field water analysis (before and after adsorption)

Parameter	Unit	Feed water	Treated Water
TDS	(mg L^{-1})	631.6±10	554.4±10
pH		7.57±0.1	7.40±0.1
Turbidity	(NTU)	4.40±0.15	1.40±0.15
As(V)	(mg L^{-1})	0.10±0.005	0.002±0.005
Fe^{3+}	(mg L^{-1})	0.00±0.03	0.00±0.03
Na^+	(mg L^{-1})	172±7.0	167±7.0
K^+	(mg L^{-1})	16.7±0.8	13.9±0.8
Mg^{2+}	(mg L^{-1})	55.80±3.0	44.60±3.0
Ca^{2+}	(mg L^{-1})	12.50±0.6	8.17±0.6
Cl^-	(mg L^{-1})	150.4±7.0	142.4±7.0
HCO_3^-	(mg L^{-1})	72.4±3.0	64.1±3.0
SO_4^{2-}	(mg L^{-1})	59.40±3.0	59.70±3.0
PO_4^{3-}	(mg L^{-1})	44.44±3.0	38.27±3.0
NO_3^-	(mg L^{-1})	33.41±3.0	25.27±3.0

Table S6 Fluoride containing field water analysis (before and after adsorption)

Parameter	Unit	Feed water	Treated Water
TDS	(mg L^{-1})	1062±10	767.4±10
pH		7.01±0.1	7.50±0.1
Turbidity	(NTU)	5.6±0.15	1.40±0.15
Na^+	(mg L^{-1})	331±10	325±10
K^+	(mg L^{-1})	37±3.0	32±3.0
Ca^{2+}	(mg L^{-1})	23±2.5	11±2.5
Fe^{3+}	(mg L^{-1})	0±0.001	0±0.001

Hg^{2+}	(mg L^{-1})	0±0.001	0±0.001
Pb^{2+}	(mg L^{-1})	0±0.001	0±0.001
HCO_3^-	(mg L^{-1})	178±7.0	160±7.0
SO_4^{2-}	(mg L^{-1})	85±5.0	74±5.0
Cl^-	(mg L^{-1})	287±7.0	267±7.0
PO_4^{3-}	(mg L^{-1})	69±3.0	57±3.0
F^-	(mg L^{-1})	7.1±0.15	0.24±0.15